Data in Brief 48 (2023) 109075

Contents lists available at ScienceDirect

Data in Brief

journal homepage: www.elsevier.com/locate/dib

Data Article

Datasets on the elastic and mechanical properties of hydroxyapatite: A first principle investigation, experiments, and pedagogical perspective

Obinna A. Osuchukwu[a,d], Abdu Salihi[a], Ibrahim Abdullahi[a], David O. Obada[b,c,d,*], Simeon A. Abolade[b,c], Akinlolu Akande[b,c], Stefan Csaki[e,g], David Dodoo-Arhin[f]

[a] *Department of Mechanical Engineering, Bayero University, Kano, 700241, Nigeria*
[b] *Mathematical Modelling and Intelligent Systems for Health and Environment Research Group, School of Science, Atlantic Technological University, Ash Lane, Ballytivnan, Sligo, F91 YW50, Ireland*
[c] *Africa Centre of Excellence on New Pedagogies in Engineering Education, Ahmadu Bello University, Zaria, 810222, Nigeria*
[d] *Multifunctional Materials Laboratory, Shell Office Complex, Department of Mechanical Engineering, Ahmadu Bello University, Zaria, 810222, Nigeria*
[e] *Department of Physics, Constantine the Philosopher University in Nitra, Nitra, 949 11, Slovakia*
[f] *Department of Materials Science and Engineering, University of Ghana, Legon, 25, Ghana*
[g] *Department of Horticultural Machinery, Faculty of Horticulture, Mendel University in Brno, Valticka 337, Lednice, 691 44, Czech Republic*

ARTICLE INFO

Article history:
Received 6 September 2022
Revised 10 March 2023
Accepted 13 March 2023
Available online 20 March 2023

Dataset link: Load and Displacement Curve Datasets for HAp samples (Original data)

ABSTRACT

The purpose of this data article is to report the quantum mechanical analysis by generalized gradient approximation (GGA) exchange-correlation functional using density functional theory (DFT). The predictions were based on the elastic constants and mechanical properties of stoichiometric hydroxyapatite (HAp) crystal. The elastic stiffness constants in hexagonal symmetry were obtained by fitting the Hookes' law for the energy-strain and stress-stain relations. Some of the theoretical datasets were compared to measured mechanical properties of produced HAp pellets obtained through micro and nanoindentation experiments. The

* Corresponding author.
E-mail address: david.obada@atu.ie (D.O. Obada).

https://doi.org/10.1016/j.dib.2023.109075

Keywords:
Hydroxyapatite
Mechanical properties
Elastic Constants
CACPLA Pedagogy
Engineering Education
Nanoindentation
Young's Modulus

datasets show considerable anisotropy in the stress-strain behaviour and are discussed in the context of the mechanical properties of HAp which are useful for tissue engineering. We also provide a pedagogical snapshot on the use of the datasets herein to teach and interpret DFT based atomistic simulations in a typical blended online teaching set-up for engineering students using a new pedagogy, CACPLA (Communicate, Active, Collaborate, Practice, Learning and Assessment).

Specifications Table

Subject	Engineering
Specific subject area	Biomedical Materials: Computational Materials Physics; Engineering Education
Type of data	Table Figure
How the data were acquired	First principle calculations Micro and nanoindentation experiments Survey links (questionnaire)
Data format	Raw Analysed (observed/experimental) and Predicted
Description of data collection	Quantum mechanical calculations from first principles DFT calculations were performed using the resources of the Trinity Centre for High Performance Computing (TCHPC), and Irish Center for High End Computing (ICHEC), Ireland Nanoindentation measurements were performed at the African University of Science and Technology (AUST), Abuja, Nigeria Usage of questionnaire to collect data from respondents (students)
Data source location	• African University of Science and Technology • Atlantic Technological University, • Africa Centre of Excellence on New Pedagogies in Engineering Education (ACENPEE) • City/Town/Region: Abuja, Zaria, and Sligo • Country: Nigeria and Ireland
Data accessibility	Repository name: 4TU. ResearchData. Data identification number: https://doi.org/10.4121/20279226.v1
Related research article	Osuchukwu, O. A., Salihi, A., Abdullahi, I., Obada, D. O., Abolade, S. A., Akande, A., & Csaki, S. (2022). Structural and Nano-Mechanical Characteristics of a Novel Mixture of Natural Hydroxyapatite Materials: Insights from Ab-initio Calculations and Experiments. *Materials Letters*, 132977. https://doi.org/10.1016/j.matlet.2022.132977

Value of the Data

- The data in this study will be useful for researchers in archiving the mechanical properties of HAp using atomistic simulations without the need to perform expensive and time-consuming experiments.
- The additional value of the datasets is inherent in the synergy between theoretically and experimentally derived mechanical properties of HAp to enable a better understanding of the mechanical behavior of HAp.
- Datasets in this work will continually justify that the improvement of reliable and accurate computational methods are important in quantum mechanical theory and will be useful for ab initio comparisons of similar materials.

• These data were used to teach and interpret DFT based atomistic simulations to engineering students using a blended online teaching and learning strategy called CACPLA.

1. Objective

These datasets were generated to add value to an ongoing research on the structural characteristics and mechanical properties of natural HAp materials on a nanoscale [1]. The data complements the results obtained in the study from a theoretical and experimental standpoint allowing a probe into the physics of the biomaterials. In addition, the outcomes of using the datasets as presented in this study for teaching a module on atomistic simulations to engineering students is highlighted.

2. Data Description

The dataset available for the calculated/atomistic simulations of the elastic constants and mechanical properties of hexagonal HAp in addition to nano and micro indentation data derived from experiments on produced HAp pellets from a mixture of two biogenic biowastes [1,2] are presented in this article. Elastic constants C_{ij}, bulk mechanical characteristics, and experimental nanoindentation measurement data for HAp are tabulated in Tables 1–3, respectively. Fig. 1 reflects the deposited raw data in the repository (4TU. ResearchData) that underlines the load and displacement curves for HAp samples obtained using nanoindentation experiments. Fig. 2 shows the Vickers hardness properties of produced HAp pellets obtained using micro indentation

Table 1
Elastic constants C_{ij} of hexagonal HAp from atomistic simulations.

	DFT Code	C_{11}(GPa)	C_{12}(GPa)	C_{13}(GPa)	C_{33}(GPa)	C_{44}(GPa)	C_{66}(GPa)
This work	VASP	117.6	34.6	72.0	162.5	44.6	41.5
Reported [3]	VASP	120.6	32.9	65.9	167.2	35.8	43.8
Reported [4]	Quantum Espresso	118.3	31.6	63.7	156.8	33.5	43.4
Reported [5]	Quantum Espresso	117.9	30.6	66.4	165.0	38.5	43.7
Reported [6]	CRYSTAL17	132.0	36.0	63.0	168.0	39.0	48.0
Reported [7]	CASTEP	139.0	49.0	61.0	178.0	47.0	45.0
Reported [8]	VASP	140.0	49.0	60.0	179.0	48.0	45.0
Reported [9]	CASTEP	149.2	52.5	64.6	180.1	41.0	48.6
Reported [10]	VASP	134.4	48.9	68.5	142.5	51.4	42.8
Reported [11]	VASP	122.2	34.4	65.2	166.6	42.1	44.4
Reported [12]	VASP	117.1	26.2	55.6	231.8	56.4	45.5

Table 2
Bulk mechanical characteristics of hexagonal HAp from atomistic simulations.

HAp (Hexagonal)	DFT Code	B (GPa)	G(GPa)	E (GPa)	B/G	υ	H_v (GPa)
This work	VASP	79.88	39.90	102.61	2.00	0.29	4.64
Reported [3]	VASP	78.84	38.83	100.05	2.03	0.29	-
Reported [4]	Quantum Espresso	76.40	37.1	95.9	2.09	0.29	-
Reported [5]	Quantum Espresso	77.00	39.40	-	1.95	-	-
Reported [6]	CRYSTAL17	82.00	43.00	110.00	1.91	0.28	-
Reported [7]	CASTEP	88.70	46.70	118.90	1.90	0.27	-
Reported [8]	VASP	86.0	-	-	-	-	-
Reported [9]	CASTEP	92.2	45.6	119.2	2.02	0.27	-
Reported [10]	VASP	-	-	-	-	-	-
Reported [11]	VASP	79.49	41.73	106.6	1.90	0.28	-
Reported [12]	VASP	76.00	52.00	-	1.46	-	-

Table 3
Experimental nano-indentation measurement data for HAp-derived pellets.

Samples	E_r (GPa)	E (GPa)
B100	0.06	0.06
C100	0.93	0.89
BC 75/25	0.79	0.76
BC 50/50	4.60	4.43
BC 25/75	4.83	4.65

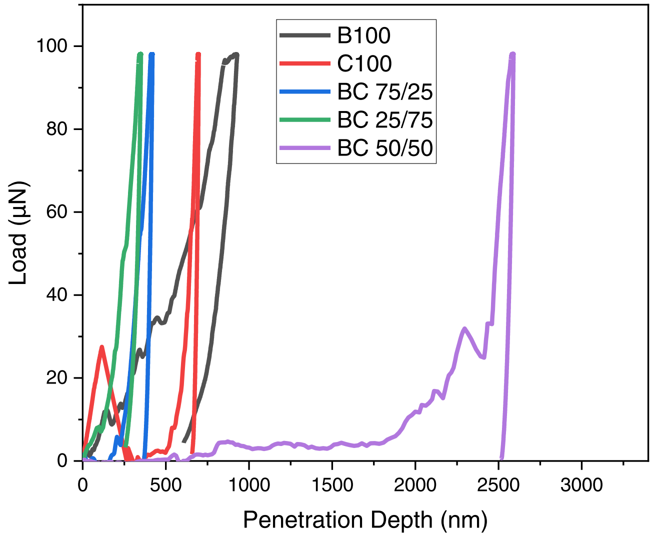

Fig. 1. Load Vs Displacement curves obtained through nanoindentation experiments for the HAp pellets.

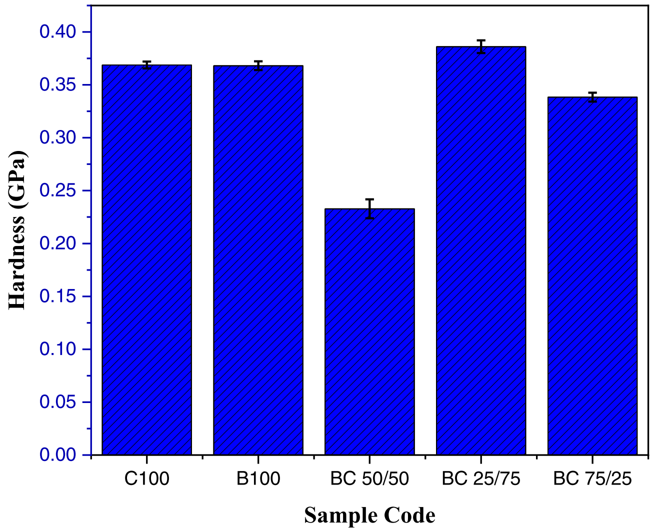

Fig. 2. Vickers hardness measurement data for the HAp pellets.

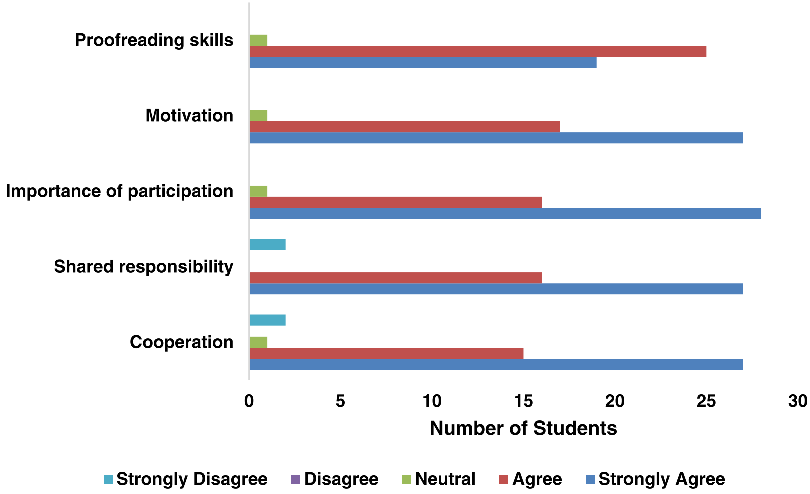

Fig. 3. Learners Satisfaction Survey (LSS) for a student sample size of N= 45.

Fig. 4. Word cloud analysis on the learners satisfaction survey.

experimentally. Figs. 3 and 4 show the learners satisfaction survey datasets and the word cloud analysis on the satisfaction survey section, respectively.

Typically, the elastic constants and bulk moduli for HAp materials are the mechanical properties that directly influences the strength of HAp scaffolds/implants. The response of the HAp crystal to applied forces on the macroscopic scale can be described by the elastic constants that explain the synergy between the mechanical and dynamical behaviour [5]. The stress and strain forces are characterized by 3 tensile and shear components resulting in 6 components. Therefore, the elastic constants produce a 6×6 symmetric matrix which includes 27 different components with 21 of these independent. However, symmetries in the crystal have the tendency to decrease the number of components. For the hexagonal crystal, there are five independent elastic constants. C_{11}, C_{12}, C_{13}, C_{33}, $C_{44} = C_{55}$ and a dependent constant $C_{66} = (C_{11} - C_{12})/2$ [4]. The elastic constants C_{11} and C_{33} describe the elasticity in length while C_{12}, C_{13}, C_{44}, and C_{66} represent the elasticity in shape. C_{11} and C_{33} are typically larger than their C_{12}, C_{13}, C_{44}, and C_{66} counterparts. Calculated ratio between bulk modulus B and shear modulus G and Poisson's ratio ν, reveal that the hexagonal HAp behaves as a ductile material.

Table 1 lists the calculated elastic constants for HAp in the study, and the estimated constants are in acceptable agreement with other computational values by other researchers [3–12]. Any significant deviation from our reported estimates can be ascribed to a variation in the description for charge and geometry of the phosphate polyhedral. The mechanical stability which was evaluated by the Born's criteria [13] reveals that the HAp crystal is mechanically stable.

The calculated estimates obtained for the elastic moduli, the ratio of B (bulk modulus) to shear modulus (G) and Poisson's ratio for the HAp crystal are tabulated in Table 2. Generally, most of the calculated elastic properties are in line with studies elsewhere [3–12]. The bulk modulus describes the resistance of the crystal to volume change when stresses are applied and can be used to measure the average bond strength of the atoms of HAp. The shear modulus describes how much resistance there is to reversible deformations over shear stress. As reported in Table 2, the B/G ratio can reveal the brittle or ductile behaviour of a material. The critical value for this separation is 1.75 [14,15]. For the HAp crystal investigated, the B/G ratio is 2.00 which is higher than 1.75 and indicates the material is ductile. This agrees with the Poisson' ratio data obtained. The Poisson ratio for ductile materials is larger than 0.26. The ductile nature of the investigated HAp crystal quantifies the stable nature of the crystal against shear deformation. The stiffness of the HAp crystal represented by the Young's modulus as calculated is 102.61 GPa and can favour the applicability of HAp in terms of mechanical characteristics such as wear and hardness when used as fillers and in restorative medicine. However, these results have been obtained in the absence of any defects in the bulk HAp crystal which could be vacancies and dislocations. Usually, these defects affect the interfacial behaviours with a direct consequence on the mechanical properties [16].

Table 3 presents the elastic deformation that occurs on the sample (HAp pellet) and the tip of the indenter which is the reduced modulus (Er), and the relationship between stress and strain during elastic deformation which is the Young's Modulus (E). The importance of E for biomedical applications cannot be overemphasized. However, there are different elastic properties of HAp found in the literature ranging from 3 to 180 GPa [12,17-22]. The factors responsible for these gradients are the porosity, morphology, crystallinity, purity, and the grain size of HAp [12,33]. Most of the reports do not report the E of HAp with a complete description of the sample characteristics in terms of the chemical composition, calcium to phosphate ratio (Ca/P), density and the structure, and this leads to a difficulty in terms of the evaluation of the datasets. The highest E reported in this study is 4.65 GPa for the BC 25/75 HAp sample and this value is comparatively lower than the E reported during atomistic simulations. This variation can be ascribed to defects in the bulk crystal during the sintering process which could cause vacancies and dislocations. Usually, these defects affect mechanical properties of the materials. The low compaction pressure used in preparing the samples and the loading during nanoindentation experiments could also cause reduced mechanical properties.

Fig. 1 represents the typical force-depth curves obtained during nanoindentation tests for the compact HAp pellets with an applied load of 100 µN, a hold time of 2 s and a loading rate of 20 µN/s. The low holding time was used to minimize the creep effect. The curve for BC 25/75 which produced the highest E was characterized by a substantial continuity, as there were no discontinuities in the curve during loading and unloading. The results indicate that E and hardness could decrease with increased loading as noticed in this study. Such characteristics could be ascribed to the indentation size effect (ISE). Typically, for higher contact loads, a larger plastic core that is generated causes some damage at the surface in the form of cracks/fractures and leads to reduced mechanical properties [23]. The Vickers microhardness data for the HAp pellets is presented in Fig. 2. The obtained micro hardness values are low as compared to microhardness (Hν) values calculated by atomistic simulations (Table 2), and this can be ascribed to defects in the bulk crystal during the sintering process and the low compaction pressure (500 Pa) used in fabricating the pellets. Higher sintering temperature could increase the mechanical characteristics of the bio-ceramics samples [24,25,26,34-37].

The learning sessions on elastic constants were accessed by the engineering students of ACENPEE through this link: https://compmatphys.epotentia.com/topic/elastic-constants-definition/. The learner's satisfaction survey link was administered to the students at the end of the teaching sessions using a five-point Likert scale with responses from strongly agree to strongly disagree as shown in Fig. 3. Forty-five (45) students with an average age of 27 participated in the survey, and from the survey plots, it can be observed that students agreed that the jigsaw approach under the collaborate section of the CACPLA pedagogy [38,39] aided their understanding of the subject and enhanced their proof-reading skills, motivation, importance of participation, shared responsibility, and cooperation amongst students in their various jigsaw groups. The percentage of students that "agreed" and "strongly agreed" to all the markers (proof reading skills, motivation etc) in the survey questions outweighs the other responses on the Likert scale. This means that when students are grouped to discuss learning outcomes, and the groups are mid-sized (in this case, 10 per group), the motivation to study, the essence of proof-reading, shared responsibility and cooperation amongst the students is enhanced, consequently impacting on their experiential learning experience. This result is also supported by the word cloud of the feedback received from the students as shown in Fig. 4. The word "good", "method", "courses", and "thank you" etc. were mentioned frequently as a result of the feedback of the students on the effectiveness of the CACPLA pedagogy and the need to apply the method to other courses. The word "network" was also mentioned frequently, and this can be ascribed to some limitations in the internet infrastructure which can be improved.

2. Experimental Design, Materials and Methods

Ab initio calculations were performed by solving density functional theory Kohn Sham equations [40]. All properties were investigated using standard Perdew-Burke-Ernzerhof (PBE) version of Generalised Gradient Approximation (GGA) alongside projector augmented wave (PAW) which was used as exchange-correlation functional as implemented in VASP [27,28] with a cutoff energy of 520 eV. Dense Monkhorst-Pack k-point meshes of 2 × 2 × 2 was utilized for the Brillouin zone sampling. The relaxation of the atoms was conducted until the atomic forces were smaller than 0.01 eV $Å^{-1}$. The initial geometry of $Ca_{10}(PO_4)_6(OH)_2$ was retrieved from the Materials Project Database (MPD). During the mechanical testing of the materials, a low cold compaction pressure of 1 MPa was used for pelletizing the sample powders. Nanoindentation was performed using the TI 950 Hysitron Tribo-Indenter at 25 °C equipped with a Berkovich tip. The peak load was 100 µN with a hold time of 2 s and a loading rate of 20 µN/s. The Young's modulus E, and hardness Hv, of the pellets were estimated using the method of Oliver and Pharr [29]. The preparation of HAp samples (powders and pellets) were produced from non-separated animal bones and catfish bones at the Multifunctional Materials Laboratory (MFML), Ahmadu Bello University, Zaria, Nigeria, which has extensive experience in synthesizing biomaterials [1,2,34,41]. The raw bones were deproteinized and subjected to heat treatment at 900 °C for 2 h. The powders produced after heat treatment were weighed and mixed in different proportions totaling 100 g. The powders were uniaxially pressed in a 25 mm diameter cylindrical die under 500 Pa compaction pressure and sintered in air atmosphere [34]. and the Vickers microhardness of the samples was determined with a microhardness tester. Young's modulus after nanoindentation was obtained from the reduced Modulus using Eq. (1) [29]

$$E = \left(1 - \upsilon^2\right)\left[\frac{1}{E_r} - \frac{1 - \upsilon_i^2}{E_i}\right]^{-1} \quad (1)$$

Where E_r is the reduced modulus, υ is the Poisson's ratio of the sample (taken as 0.2 for ceramics), E_i is the Young's Modulus of the indenter (taken as 1,141 GPa or 1,141,000 MPa for diamond), and υ_i is the Poisson's ratio of the indenter (taken as 0.07 for diamond).

The elastic constants are described by the stress-strain relation for the hexagonal structures:

$$\begin{bmatrix} \sigma_1 \\ \sigma_2 \\ \sigma_3 \\ \sigma_4 \\ \sigma_5 \\ \sigma_6 \end{bmatrix} = \begin{bmatrix} C_{11} & C_{12} & C_{13} & 0 & 0 & 0 \\ C_{12} & C_{11} & C_{13} & 0 & 0 & 0 \\ C_{13} & C_{13} & C_{33} & 0 & 0 & 0 \\ 0 & 0 & 0 & C_{44} & 0 & 0 \\ 0 & 0 & 0 & 0 & C_{44} & 0 \\ 0 & 0 & 0 & 0 & 0 & C_{66} \end{bmatrix} \begin{bmatrix} \varepsilon_1 \\ \varepsilon_2 \\ \varepsilon_3 \\ \varepsilon_4 \\ \varepsilon_5 \\ \varepsilon_6 \end{bmatrix}$$

$$C_{66} = (C_{11} - C_{12})/2$$

To describe polycrystalline constants, there are three types of algorithms which corresponds to different bounds and are based on the elastic constant of a single crystal. Voigt and Reuss expressed stress in terms of a given strain and the strain in terms of the given stress, respectively. Hill established that approximations made by Voigt [30] and Reuss [31] consider the upper and lower bounds of the elastic constants, respectively. Hence, Hills' [32] averages are used to predict bulk (B) and shear (G) moduli of the polycrystalline aggregates. For hexagonal structures, these equations Eqs. 2-(7) are:

$$B_\nu = \frac{1}{9}[2(C_{11} + C_{44}) + C_{33} + 4C_{13}], \tag{2}$$

$$G_\nu = \frac{1}{30}[7C_{11} - 5C_{12} + 12C_{44} + 2C_{33} - 4C_{13}], \tag{3}$$

$$B_R = \left[(C_{11} + C_{12})C_{33} - 2C_{13}^2\right] / [C_{11} + C_{12} + 2C_{33} - 4C_{13}], \tag{4}$$

$$G_R = \frac{5}{2}\left\{\left[[C_{11} + C_{12})C_{33} - 2C_{13}^2\right]C_{44}\,C_{66}]/[3B_\nu C_{44}\,C_{66} + \left[(C_{11} + C_{12})C_{33} - 2C_{13}^2\right](C_{44} + C_{66})]\right\}, \tag{5}$$

Hill's averages are used to predict bulk (B) and shear (G) moduli

$$B = \frac{1}{2}(B_R + B_\nu) \text{ and } G = \frac{1}{2}(G_R + G_\nu) \tag{6}$$

The Young's modulus (E) and Poisson's ratio (ν), major elasticity-related parameters are given by the following formulas:

$$E = \frac{9GB}{3B + G} \text{ and } \nu = \frac{3B - 2G}{2(3B + G)} \tag{7}$$

To evaluate the mechanical stability, the Born stability criteria [13] is used as shown in Eq. 8:

$$C_{11} > |C_{12}|, \ (C_{11} + 2C_{12})C_{33} > 2C_{13}^2,$$

$$C_{44} > 0, \tag{8}$$

The students were asked to watch a video and study the downloadable slides at: https://compmatphys.epotentia.com/topic/elastic-constants-definition/ Next, the students were split into 7 groups of 10 students each to discuss subtopics per the Jigsaw Strategy, and specific tasks were allotted.

Each group was assigned a subtopic under elasticity as follows:

Group 1: Stress and strain in engineering materials
Group 2: Elastic Hysteresis
Group 3: Hooke's law
Group 4: Stress Tensors

Group 5: Bulk Modulus
Group 6: Modulus of Elasticity
Group 7: Young Modulus

Each group was expected to come up with three power point slides that summarizes the core concept of the subtopics assigned. This way, when the slides (jigsaw pieces) were put together by the overall champions of all groups, it gives a full picture of elasticity. The learners satisfaction survey (LSS) questionnaires were designed to understand the opinion of the students on the impact of the jigsaw strategy (a part of the collaborate section of the CACPLA pedagogy) used during the blended online teaching and learning strategy. The LSS was made using the google form and composed mainly of Likert scale questions that required the participants to indicate their level of agreement or disagreement on statements that cover general feedback on the various aspects of the strategy used. The questionnaire was based on a 5-point Likert scale which is as follows: 1 (strongly disagree), 2 (disagree), 3 (neutral), 4 (agree), and 5 (strongly agree).

Ethics Statements

Students filled in a consent form, and the learners satisfaction survey link which was was administered to the students used a five-point Likert scale through the use of google forms.

Declaration of Competing Interest

The authors declare that they have no known competing financial interests or personal relationships that could have appeared to influence the work reported in this paper.

Data Availability

Load and Displacement Curve Datasets for HAp samples (Original data) (4TU.ResearchData).

CRediT Author Statement

Obinna A. Osuchukwu: Methodology, Data curation; **Abdu Salihi:** Supervision; **Ibrahim Abdullahi:** Supervision; **David O. Obada:** Conceptualization, Methodology, Data curation, Writing – original draft, Investigation, Writing – review & editing, Supervision; **Simeon A. Abolade:** Methodology, Data curation; **Akinlolu Akande:** Writing – review & editing, Supervision; **Stefan Csaki:** Writing – review & editing; **David Dodoo-Arhin:** Writing – review & editing.

Funding Statement

The authors wish to acknowledge funding from Tertiary Education Trust Fund (TETFund), Nigeria under grant Ref: NRF_SETI_HSW_00714, 2020, and the Africa Centre of Excellence on New Pedagogies in Engineering Education

Acknowledgments

The authors acknowledge the Multifunctional Materials Laboratory, Shell Office in Mechanical Engineering, Ahmadu Bello University, Zaria, Nigeria, the Department of Metallurgical and Materials Engineering, Ahmadu Bello University, Zaria, Nigeria and the Department of Mechanical Engineering, Bayero University, Kano, Nigeria, for providing facilities to carry out this study.

In addition, the authors acknowledge the Tertiary Education Trust Fund (TETFund) in Nigeria for funding this study under the National Research Fund category with grant reference: NRF_SETI_HSW_00714, 2020, and the Irish Research Council for funding granted to DOO with Project ID GOIPD/2021/28. SAA thanks the Atlantic Technological University, Sligo, President Bursary Award for funding support. Most of the calculations were performed on the Kelvin cluster maintained by the Trinity Centre for High Performance Computing (TCHPC) (Project codes: HPC_22_01254 and HPC_21_01219). This cluster was funded through grants from the Higher Education Authority, through its PRTLI program. The authors also wish to acknowledge the Irish Centre for High-End Computing (ICHEC) (Project codes: isphy005c and isphy006c) for the provision of computational facilities and support.

References

[1] O.A. Osuchukwu, A. Salihi, I. Abdullahi, D.O. Obada, S.A. Abolade, A. Akande, S. Csaki, Structural and Nano-Mechanical Characteristics of a Novel Mixture of Natural Hydroxyapatite Materials: Insights from Ab-initio Calculations and Experiments, Mater. Lett. (2022) 132977.
[2] O.A. Osuchukwu, A. Salihi, I. Abdullahi, D.O. Obada, Experimental data on the characterization of hydroxyapatite produced from a novel mixture of biowastes, Data Brief (2022) 108305.
[3] W. Sailuam, K. Phacheerak, I. Fongkaew, S. Limpijumnong, Elastic and mechanical properties of hydroxyapatite under pressure: A first-principles investigation, J Phys Condens Matter 24 (2020) e00481.
[4] S.S. Bhat, U.V. Waghmare, U. Ramamurty, First-principles study of structure, vibrational, and elastic properties of stoichiometric and calcium-deficient hydroxyapatite, Cryst. Growth Des. 14 (6) (2014) 3131–3141.
[5] E. Menendez-Proupin, S. Cervantes-Rodríguez, R. Osorio-Pulgar, M. Franco-Cisterna, H. Camacho-Montes, M.E. Fuentes, Computer simulation of elastic constants of hydroxyapatite and fluorapatite, J. Mech. Behav. Biomed. Mater. 4 (7) (2011) 1011–1020.
[6] M. Wang, H.Y. Zhang, Y.Y. Xiang, Y.P. Qian, J.N. Ren, R. Jia, How does fluoride enhance hydroxyapatite? A theoretical understanding, Appl. Surf. Sci. 586 (2022) 152753.
[7] K. Moradi, A.A. Sabbagh Alvani, First-principles study on Sr-doped hydroxyapatite as a biocompatible filler for photo-cured dental composites, J. Aust. Ceram. Soc. 56 (2) (2020) 591–598.
[8] K. Kawabata, T. Yamamoto, First-principles calculations of the elastic properties of hydroxyapatite doped with divalent ions, J. Ceram. Soc. Jpn. 118 (1378) (2010) 548–549.
[9] Q. Yuan, L. Wan, J. Wu, A. Xu, Investigation of the effect of doped Zn atom to the hydroxyapatite based on experimental method and first-principles calculations, J. Aust. Ceram. Soc. 56 (4) (2020) 1413–1419.
[10] N.H. de Leeuw, J.R. Bowe, J.A. Rabone, A computational investigation of stoichiometric and calcium-deficient oxy-and hydroxy-apatites, Faraday Discuss. 134 (2007) 195–214.
[11] S. Aryal, K. Matsunaga, W.Y. Ching, Ab initio simulation of elastic and mechanical properties of Zn-and Mg-doped hydroxyapatite (HAP), J. Mech. Behav. Biomed. Mater. 47 (2015) 135–146.
[12] R. Snyders, D. Music, D. Sigumonrong, B. Schelnberger, J. Jensen, J.M. Schneider, Experimental and ab initio study of the mechanical properties of hydroxyapatite, Appl. Phys. Lett. 90 (19) (2007) 193902.
[13] M. Born, Dynamical theory of crystal lattices K. Huang, Oxford University Press, 1954.
[14] D.L. Pu, Y. Pan, Influence of high pressure on the structure, hardness, and brittle-to-ductile transition of NbSi2 ceramics, Ceram. Int. 47 (2) (2021) 2311–2318.
[15] M. Wang, C. Xia, Y. Wu, D. Chen, Z. Chen, N. Ma, H. Wang, Phase stability, elastic and electronic properties of Hf–Rh intermetallic compounds from first-principles calculations, RSC Adv. 7 (33) (2017) 20241–20251.
[16] L. Wang, H.W. Zhang, X. Deng, Influence of defects on mechanical properties of bicrystal copper grain boundary interfaces, J. Phys. D Appl. Phys. 41 (13) (2008) 135304.
[17] R.S. Gilmore, J.L. Katz, Elastic properties of apatites, J. Mater. Sci. 17 (4) (1982) 1131–1141.
[18] H.J.A. Van Dijk, N. Hattu, K. Prijs, Preparation, microstructure and mechanical properties of dense polycrystalline hydroxy apatite, J. Mater. Sci. 16 (6) (1981) 1592–1598.
[19] M.A. Lopes, R.F. Silva, F.J. Monteiro, J.D. Santos, Microstructural dependence of Young's and shear moduli of P_2O_5 glass reinforced hydroxyapatite for biomedical applications, Biomaterials 21 (7) (2000) 749–754.
[20] Y.C. Yang, E. Chang, B.H. Hwang, S.Y. Lee, Biaxial residual stress states of plasma-sprayed hydroxyapatite coatings on titanium alloy substrate, Biomaterials 21 (13) (2000) 1327–1337.
[21] B. León, Pulsed laser deposition of thin calcium phosphate coatings, Thin Calcium Phosphate Coatings Med. Implants (2009) 101–155.
[22] V. Nelea, H. Pelletier, M. Iliescu, J. Werckmann, V. Craciun, I.N. Mihailescu, … C. Ghica, Calcium phosphate thin film processing by pulsed laser deposition and in situ assisted ultraviolet pulsed laser deposition, J. Mater. Sci. Mater. Med. 13 (12) (2002) 1167–1173.
[23] C.Y. Tang, P.S. Uskokovic, C.P. Tsui, D. Veljovic, R. Petrovic, D. Janackovic, Influence of microstructure and phase composition on the nanoindentation characterization of bioceramic materials based on hydroxyapatite, Ceram. Int. 35 (6) (2009) 2171–2178.
[24] D.O Obada, K.A Salami, A.N Oyedeji, O.O Fasanya, M.U Suleiman, B.A Ibisola, … E.T Dauda, Solution combustion synthesis of strontium-doped hydroxyapatite: effect of sintering and low compaction pressure on the mechanical properties and physiological stability, Mater. Lett. 304 (2021) 130613.

[25] D.O. Obada, S.A. Osseni, H. Sina, K.A. Salami, A.N. Oyedeji, D. Dodoo-Arhin, … E.T. Dauda, Fabrication of novel kaolin-reinforced hydroxyapatite scaffolds with robust compressive strengths for bone regeneration, Appl. Clay Sci. 215 (2021) 106298.
[26] D.O. Obada, D. Dodoo-Arhin, M. Dauda, F.O. Anafi, A.S. Ahmed, O.A. Ajayi, Physico-mechanical and gas permeability characteristics of kaolin based ceramic membranes prepared with a new pore-forming agent, Appl. Clay Sci. 150 (2017) 175–183.
[27] G. Kresse, J. Furthmüller, Efficient iterative schemes for ab initio total-energy calculations using a plane-wave basis set, Phys. Rev. B 54 (16) (1996) 11169.
[28] JP Perdew J.P. Perdew, K. Burke, M. Ernzerhof, Phys Rev Lett 77 (1996) 3865.
[29] W.C. Oliver, G.M. Pharr, An improved technique for determining hardness and elastic modulus using load and displacement sensing indentation experiments, J. Mater. Res. 7 (6) (1992) 1564–1583.
[30] Voigt, W. (1928). Lehrbuch der Kristallphysik, Lehrbuch der Kristallphysik.
[31] A.J.Z.A.M.M. Reuss, Calculation of the flow limits of mixed crystals on the basis of the plasticity of monocrystals, Z Angew Math Mech 9 (1929) 49–58.
[32] R. Hill, The elastic behaviour of a crystalline aggregate, Proc. Phys. Soc. London Sect. A 65 (5) (1952) 349.
[33] O.A. Osuchukwu, A. Salihi, I. Abdullahi, D.O. Obada, Synthesis and characterization of sol–gel derived hydroxyapatite from a novel mix of two natural biowastes and their potentials for biomedical applications, Materials Today: Proceedings, 2022.
[34] D.O. Obada, E.T. Dauda, J.K. Abifarin, D. Dodoo-Arhin, N.D. Bansod, Mechanical properties of natural hydroxyapatite using low cold compaction pressure: Effect of sintering temperature, Mater. Chem. Phys. 239 (2020) 122099.
[35] E.S. Akpan, M. Dauda, L.S. Kuburi, D.O. Obada, D. Dodoo-Arhin, A comparative study of the mechanical integrity of natural hydroxyapatite scaffolds prepared from two biogenic sources using a low compaction pressure method, Results Phys. 17 (2020) 103051.
[36] D.O. Obada, E.T. Dauda, J.K. Abifarin, N.D. Bansod, D. Dodoo-Arhin, Mechanical measurements of pure and kaolin reinforced hydroxyapatite-derived scaffolds: a comparative study, Mater. Today 38 (2021) 2295–2300.
[37] E.S. Akpan, M. Dauda, L.S. Kuburi, D.O. Obada, Box-Behnken experimental design for the process optimization of catfish bones derived hydroxyapatite: A pedagogical approach, Mater. Chem. Phys. 272 (2021) 124916.
[38] D.O. Obada, R.B. Bako, A.S. Ahmed, F.O. Anafi, A.O. Eberemu, D. Dodoo-Arhin, … I.B. Obada, Teaching bioengineering using a blended online teaching and learning strategy: a new pedagogy for adapting classrooms in developing countries, Educ. Inf. Technol. (2022) 1–24.
[39] A.O. Eberemu, D.O. Obada, R.B. Bako, A.S. Ahmed, F.O. Anafi, K.J. Osinubi, Enhancing the Interest of Undergraduate Students in Geotechnical Engineering Using the CACPLA Pedagogy, In Geo-Congress (2022) 534–543.
[40] P. Hohenberg, W.J.P.R. Kohn, Density functional theory (DFT), Phys Rev 136 (1964) B864.
[41] E.S. Akpan, M. Dauda, L.S. Kuburi, D.O. Obada, A facile synthesis method and fracture toughness evaluation of catfish bones-derived hydroxyapatite, MRS Adv. 5 (26) (2020) 1357–1366.